3D Finite Element Modeling to Study the Behavior of Shape Memory Alloy Confined Concrete

Q. Chen & B. Andrawes
University of Illinois at Urbana-Champaign, USA

SUMMARY:
The application of Shape Memory Alloy (SMA) spirals to provide confinement for concrete has been proven to greatly increase the strength and ductility of concrete elements. This paper proposes a plasticity model to predict the behavior of SMA confined concrete under monotonic compression. SMA confinement behaves as a combination of active and passive confinement. This plasticity model is calibrated within the framework of damaged plasticity model, including yield criterion, hardening/softening function, and flow rule. Flow rule and hardening/softening function, which depend on confinement type, lateral confining pressure and plastic deformation, are proposed based on previous test results. Finite element analyses of concrete cylinders confined with SMA spirals and hybrid wraps made of SMA and FRP show good agreement with experimental results.

Keywords: *Shape Memory Alloys, Confinement, Concrete, Finite Element, Damaged Plasticity Model*

1. INTRODUCTION

Lateral concrete confinement is commonly used to delay the failure of concrete and improve its ductility; a feature that is critically important for structures subjected to extreme loads such as earthquakes. There are mainly two types of lateral confinement techniques, namely passive confinement and active confinement. Passively confined concrete relies on the use of the confining pressure developed during loading due to the dilation of concrete, which mobilizes the wraps/reinforcement; while active confinement is induced by applying lateral confining pressure to concrete prior to loading, i.e. applying prestress in the transverse direction. Due to the initial confining pressure before loading, active confinement can effectively delay the dilation of concrete and hence is more efficient in increasing concrete compressive strength and ultimate strain than passive confinement. Due to the limitation and challenges (requires too much labor, time and hence increases the cost) in applying prestress in steel strips, strands and fiber reinforced polymer (FRP) straps, the application of active confinement using conventional materials such as steel and FRP is limited. Shin and Andrawes (2010) used SMA spirals to actively confine concrete through thermal prestressing, which demonstrates more promising features in practical application to both new structures and retrofitting of old structures. In this application, active confining pressure is applied by simply heating prestrained SMA spirals up to above a specific temperature known as the austenite finish temperature. The behavior of SMA confined concrete is quite different from purely active or passive confinement. Due to the relatively large stiffness of the prestressed spirals, SMA confined concrete works as a combination of actively and passively confined concrete. This paper presents a damaged plasticity model to predict and analyze the behavior of concrete confined by SMA spirals using finite element (FE) method, aiming to validate this numerical modeling technique by using previous test results from different confinement techniques. Numerical modeling in this paper was conducted using ABAQUS within the framework of Concrete Damaged Plasticity Model.

2. SMA CONCRETE CONFINEMENT

2.1. Shape Memory Effect

SMA is kind of metallic alloys characterized by the shape memory effect (SME) and superelasticity (SE); two unique thermo-mechanical phenomena which enable SMA to recover its original shape through phase transformation between austenite and martensite phases. The phase transformation is governed by four transformation temperatures, namely martensite finish temperature M_f, martensite start temperature M_s, austenite start temperature A_s, and austenite finish temperature A_f. SME is the phenomenon utilized in the SMA confinement technique discussed in this paper. Fig.1 illustrates the phenomenon of SME; when the martensitic SMA wire is not restrained and is deformed under an applied force, it can recover its original shape when heated to a temperature above A_f. If the SMA wire is restrained, hence not able to recover its original length, a recovery stress will develop in the wire. In order to utilize this phenomenon in confining concrete elements, SMA wires (approximately 6% prestrained by the manufacturer) are first wrapped around the concrete element, and then heated to a temperature above A_f to activate the shape recovery. Due to the constraint provided by the concrete, the spiral is not able to restore its original length; rather a large recovery stress is induced in the spiral causing the confining pressure to be exerted on the concrete. Shin and Andrawes (2010) have explored experimentally the behavior of SMA confined concrete using SME. They also applied this technique in seismic retrofitting and repair of RC bridge piers (Shin and Andrawes 2011).

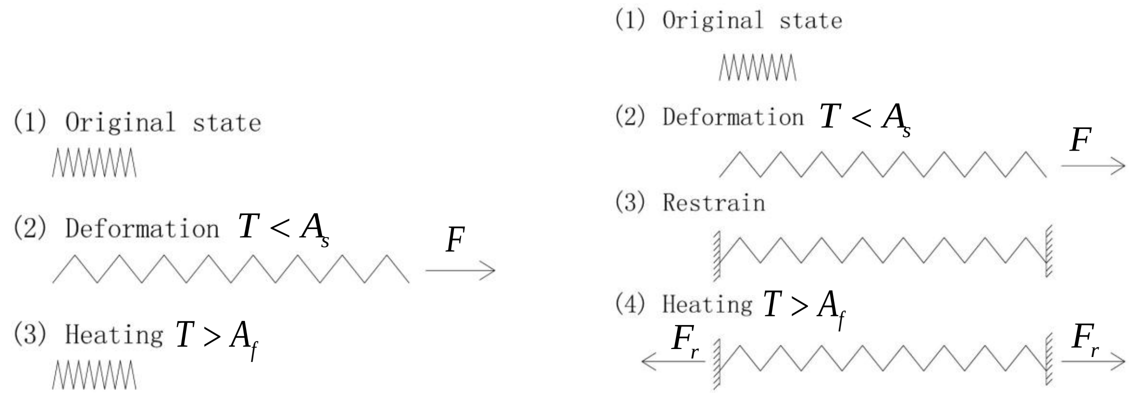

(a) Unrestrained ends (F is applied force) (b) Restrained ends (F_r is recovery force)

Figure 1. Shape memory effect of SMA

To efficiently use this SME in concrete confinement, it requires SMA to have a wide thermal hysteresis such that the transformation from martensite to austenite does not occur at typical ambient temperatures. This feature is important for the prestrained spiral to maintain its deformation until the installation is complete and the spiral is heated. To satisfy this condition, the NiTiNb alloy was utilized in this study due to its wide thermal hysteresis. As stated earlier, the behavior of SMA confined concrete is different from purely active or purely passive confinement in the sense that prior to concrete loading, recovery stress in the spiral actively confines concrete. During loading, concrete dilates laterally and additional passive confining pressure is exerted on the concrete element. Fig. 2 displays the recovery stress test results of a restrained SMA wire with 6.4% prestrain from Shin and Andrawes (2010). Before the cyclic loading was applied, recovery stress was induced in the wire through heating. When the SMA wire was subjected to cyclic loading after the recovery stress became stable, additional stress developed in the wire. Due to this unique characteristic, SMA confined concrete requires a new modeling technique to analyze the behavior, which is different from steel reinforcement, FRP or purely active confined concrete model in previous researches.

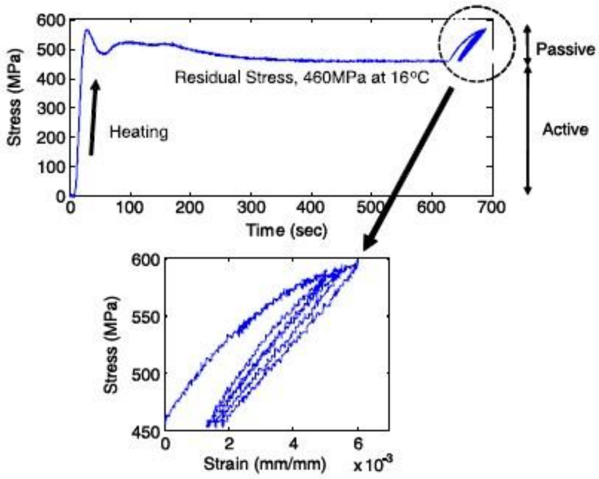

Figure 2. Recovery stress test by Shin and Andrawes (2010)

2.2. Active and Passive Confining Pressure Calculation

Mander *et al.* (1988) described the lateral confining pressure of circular section from transverse reinforcement using the following expression:

$$f_l = 2 f_h A_{sp} / s d_s \tag{2.1}$$

where f_h is transverse reinforcement hoop stress; A_{sp} is transverse reinforcement cross section area; f_l is lateral confining pressure; d_s is diameter of cylinder; s is pitch of spiral. According to Mander *et al.* (1988), this confining pressure cannot be fully achieved due to arching effect and it has to be reduced by a confinement effectiveness coefficient k_e to attain effective confining pressure $f_l^{'}$. The effective active confining pressure from SMA spirals can be calculated using recovery stress for the hoop stress in Eqn. 2.1 and the confinement effectiveness coefficient k_e proposed by Mander *et al.* (1988). However, the maximum recovery stress obtained from a recovery stress test using a straight wire cannot be totally achieved. Shin and Andrawes (2010) demonstrated that there were prestress losses when SMA spirals are heated, due to the geometric imperfection of the spirals. Therefore, active hoop stress along spirals is equal to the residual recovery stress after prestrain loss.

Passive confining pressure is calculated using hoop stress developing in the SMA spirals during loading. In order to obtain the hoop stress along spirals when concrete dilates, tensile test results of SMA wires are used. Teng *et al.* (2007) proposed an equation to describe the lateral-axial strain relationship of unconfined, actively confined and FRP confined concrete, which depends on the current confining ratio ($\sigma_l / f_{co}^{'}$).This equation is adopted in the modeling of SMA and GFRP-SMA hybrid confined concrete due to its ability to model both active and passive confinement. The expression of the lateral-axial strain relationship is as follows.

$$\frac{\varepsilon_c}{\varepsilon_{co}} = 0.85\left(1+8\frac{\sigma_l}{f_{co}^{'}}\right)\left\{\left[1+0.75\left(\frac{-\varepsilon_l}{\varepsilon_{co}}\right)\right]^{0.7} - \exp\left(-7\left(\frac{-\varepsilon_l}{\varepsilon_{co}}\right)\right)\right\} \tag{2.2}$$

where σ_l is current confining pressure; $f_{co}^{'}$ is unconfined concrete strength; ε_c is axial strain; ε_{co} is strain corresponding to unconfined peak concrete stress; ε_l is lateral strain (positive is for compression).

Previous researchers modeled FRP confined concrete stress-strain curves based on a series of active confinement stress-strain curves (Mirmiran and Shahawy 1996; Chun and Park 2002; Teng *et al.* 2007), with an assumption that each point on the stress-strain curve of FRP confined concrete is corresponding to a point on the active confinement stress-strain curve with the same lateral confining pressure as provided by FRP jacket. This paper extends this concept to SMA confined concrete. Fig. 3 shows the intersection between SMA confined concrete stress-strain test result (Shin and Andrawes 2010) and a set of actively confined concrete stress-strain curves with different confining pressures (based on Mander *et al.* 1988). The figure illustrates that the initial response of SMA confined concrete follows the path of actively confined concrete stress-strain curve with confining pressure similar to the initial active confining pressure from SMA spirals. This active confining pressure is equal to 1.42 MPa for this test based on Eqn. 2.1. During loading, as concrete dilates, SMA confined concrete stress-strain curve intersects those actively confined concrete stress-strain curves sequentially as the confining pressure increases. Therefore, one can assume that each point on the axial stress-strain curve of SMA confined concrete is corresponding to a point on the actively confined concrete axial stress-strain curve with the same lateral confining pressure as provided by the SMA spirals.

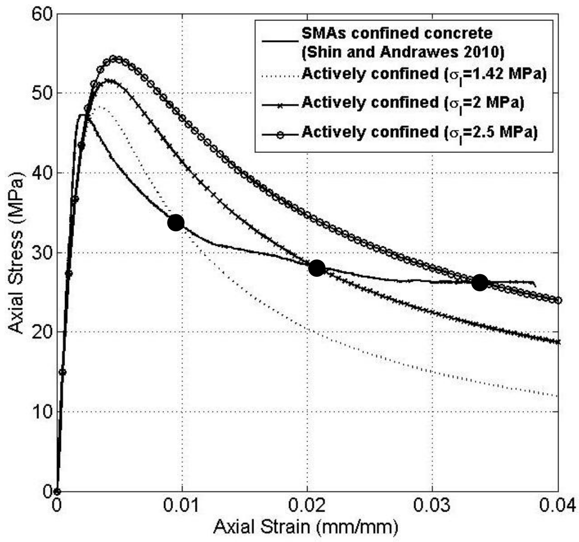

Figure 3. Intersection of several actively confined concrete stress-strain curves with SMA confined concrete test result

3. Damaged Plasticity Model

Plasticity models are characterized by three important components, namely yield criterion, flow rule, and hardening/softening function. Lubliner *et al.* (1989) proposed a plastic-damage model for concrete to include the effect of stiffness degradation in the nonlinearity of concrete behavior, which was modified by Lee and Fenves (1998) to account for different stiffness degradations in tension and in compression. This model is adopted in ABAQUS as Concrete Damaged Plasticity Model. In the present paper, numerical modeling of SMA confinement and GFRP-SMA confinement is conducted within the framework of Concrete Damaged Plasticity Model in ABAQUS, with an assumption that the nonlinearity of concrete is due to plasticity only, i.e. damage variable is equal to zero.

3.1. Yield Criterion

The yield criterion described in Lubliner *et al.* (1989) and modified in Lee and Fenves (1998) is used. This yield function reduces to Drucker-Prager yield function when concrete is in triaxial compression (Yu *et al.* 2010) as given by the following function:

$$\sqrt{J_2} + \theta I_1 - k = 0 \tag{3.1}$$

where J_2 and I_1 are second deviatoric stress invariant and first stress invariant, respectively; θ is frictional angle and its calculation was described in Oh (2002); k is hardening/softening function.

The parameter K_c, which is one of the input parameter in the damaged plasticity model, is defined as the ratio of second stress invariant on the tensile meridian to that on the compressive meridian at initial yield for a given first stress invariant. K_c represents the effectiveness of lateral confining pressure in improving shear strength and it decreases as the effectiveness of confining pressure increases. Different tests revealed different values of K_c (0.69 from Richart *et al.* 1928; 0.64 from Schickert and Winkler 1977; 0.725 from Teng *et al.* 2007). For SMA confined concrete, based on Mander *et al.* (1988) model, K_c was found to be equal to 0.64. For GFRP-SMA confined concrete, a modified K_c should be utilized, as a result of the presence of GFRP jacket between SMA spirals and concrete, which reduces the effectiveness of SMA confinement, which was verified by the experimental results from Shin and Andrawes (2010). The SMA confined concrete cylinder with 13mm-pitch spirals reached peak strength of 47.3 MPa, while the hybrid case with the same pitch of SMA spirals and 4 layers of GFRP between concrete and SMA spirals only achieved 42.6 MPa. The presence of GFRP between concrete and SMA spirals reduces the peak strength by 10%. K_c factor needs to be modified before GFRP jacket ruptures, but no modification is adopted after the rupture of GFRP jacket to consider the direct contribution from SMA spirals. Through trial and error, a value of 0.8 was adopted before GFRP ruptures for the current test. It is important to note that more tests are needed to explore how the FRP jacket presence between concrete and SMA spirals affects K_c factor.

3.2. Hardening/Softening Function

A series of hardening/softening functions are calculated using Mander *et al.* (1988) model, since this model was calibrated using William and Warnke yield surface (1975) based on Schickert and Winkler (1977) triaxial test results, which was proposed for actively confined concrete behavior. Fig. 4(a) displays a series of hardening/softening functions based on Mander *et al.* (1988) model, which were used in the simulation of SMA and GFRP-SMA confined concrete.

3.3. Flow Rule

Flow rule is described by potential flow function. The following Drucker-Prager type potential function is used in this model:

$$G = \sqrt{J_2} + \left(\alpha / 6\right) I_1 \tag{3.2}$$

where α is dilation angle. In order to describe the potential flow, a series of confining pressure dependent dilation angle functions are calculated using Mander *et al.* (1988) model as given in the following equation (Oh 2002).

$$\alpha = \sqrt{3}\,\frac{\Delta\varepsilon_c^p + 2\Delta\varepsilon_l^p}{\left|\Delta\varepsilon_c^p - \Delta\varepsilon_l^p\right|} \tag{3.3}$$

where $\Delta\varepsilon_c^p$ is incremental axial plastic strain; $\Delta\varepsilon_l^p$ is incremental lateral plastic strain.

Fig. 4(b) displays a series of dilation angle functions based on Mander *et al.* (1988), which is used in the simulation of SMA confined concrete and GFRP-SMA confined concrete.

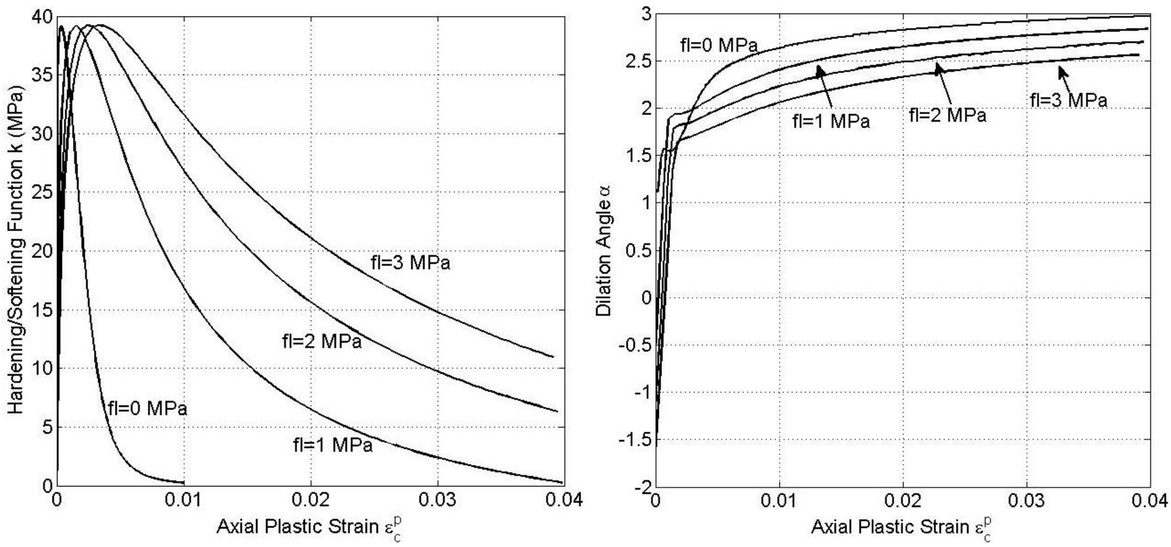

(a) (b)

Figure 4. (a) Hardening/Softening functions; (b) Dilation angle functions

4. FINITE ELEMENT ANALYSIS

To validate the damaged plasticity model proposed in this study, finite element method was utilized to model the concrete cylinder specimens tested by Shin and Andrawes (2010). They investigated the behavior of SMA confined concrete and GFRP-SMA confined concrete by testing a number of 152mm×305mm concrete cylinders in uniaxial compression. Fig .5 shows the SMA confined concrete cylinder specimen before, during and after testing. Two types of wraps described in their tests are modeled in this paper using Concrete Damaged Plasticity Model in ABAQUS: (1) SMA spirals with 13 mm pitch spacing, (2) hybrid wraps with 4 layers of GFRP and 13 mm pitch spacing SMA wrapped on the top of the GFRP. SMA wire had a diameter of 2 mm and each layer of GFRP sheet had a thickness of 0.11 mm. The elastic modulus and ultimate strain of GFRP were 19000 MPa and 0.018 mm/mm, respectively. The FE model is described in the next section.

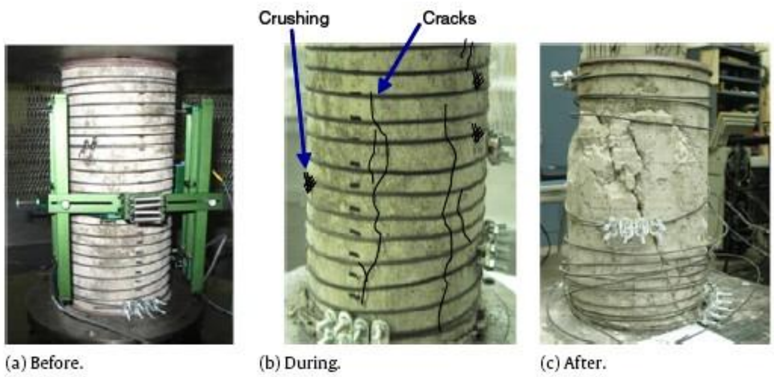

Figure 5. SMA confined concrete cylinder test by Shin and Andrawes (2010)

4.1. FE Model Description

For both SMA confinement and GFRP-SMA hybrid confinement models, concrete is modeled by 8-node solid elements and SMA spirals are modeled by 2-node truss elements. SMA spirals property is based on SMA wire tensile coupon test result after stress recovery. 4-node shell elements are used for FRP jacket. FRP jacket is assumed to have linear elastic behavior until rupture. The failure surface is represented by Von Mises Criterion with failure stress calculated from the tensile rupture strain reduced by an efficiency factor of 0.5. This efficiency factor is based on previous research (Xiao and Wu 2000) and it considers the circular shape of FRP jacket in the cylinder test and the local stress concentration from the concrete damaged underneath the jacket. The interactions between concrete and SMA spirals, between GFRP and SMA spirals are modeled by tie constraint in ABAQUS, which ties the nodes from one surface to the corresponding node in the contact surface, and the two tied nodes maintain the same displacements. This assumes slippage between two contact surfaces is negligible. Fig. 6(a) shows the FE mesh for SMA confined concrete model.

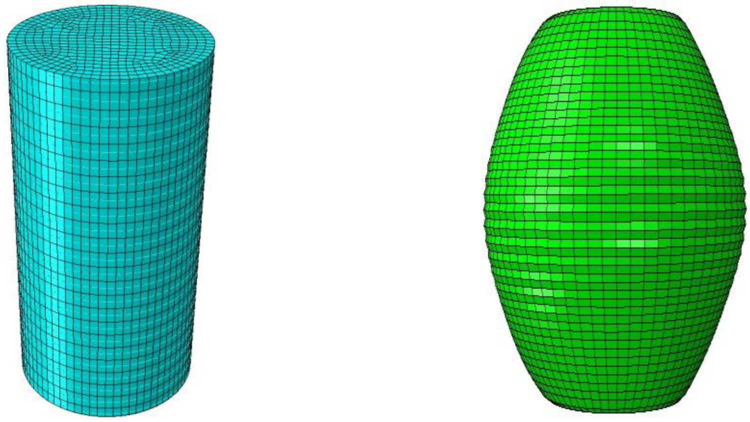

(a) (b)

Figure 6. (a) FE mesh for SMA confined concrete model; (b) SMA confined concrete cylinder deformation during loading

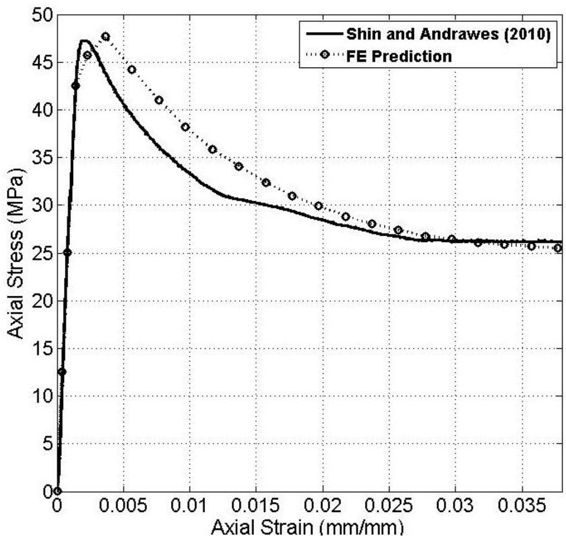

Figure 7. FE prediction of SMA confined concrete compared with experimental result

4.2. Numerical Results and Analysis

4.2.1. SMA confinement

Fig. 7 shows a comparison between the experimental and numerical (FE) prediction of the stress-strain behavior of SMA confined concrete. The proposed model can capture the peak strength and the softening branch of the axial stress-strain curve in an acceptable accuracy. The prediction of the peak stress is 47.7 MPa, while the experimental result is 47.3 MPa (0.8% difference). In addition, since hardening/softening function and flow rule are calibrated from a series of actively confined concrete stress-strain and lateral-axial strain curve under different confining pressures, one can conclude that the assumption that each point on the axial stress-strain curve of SMA confined concrete corresponds to a point on the actively confined concrete axial stress-strain curve with the same lateral confining pressure provided by SMA spirals is valid. Fig. 6(b) demonstrates the FE results of SMA confined concrete cylinder deformation during loading.

Fig. 8 shows the evolution of confining pressure at mid-height of concrete cylinder under the spiral after active confinement is applied and while the axial load is being applied. Confining pressure is uniformly distributed in the circumferential direction. As the applied axial load increases, confining pressure increases in the diametric direction towards the concrete core. Hence, core concrete is more confined than surface concrete and cover concrete starts to crack as axial loading becomes larger.

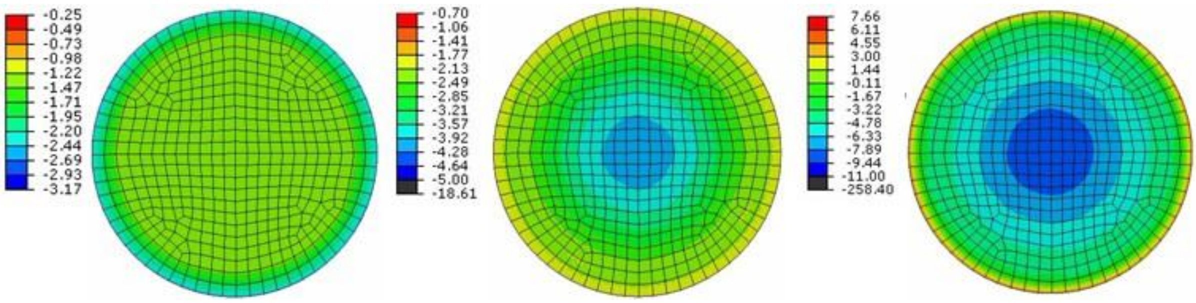

(a) (b) (c)

Figure 8. Evolution of confining pressure (MPa) (a) after active confining pressure is applied and before axial load application; (b) when axial strain is 0.004 mm/mm; (c) when axial strain is 0.014 mm/mm

Mander *et al.* (1988) used arching action to explain the ineffectively confined region appearing between spirals with a parabolic shape. Assuming that the volume of concrete with active confining pressure less than the value calculated by Eqn. 2.1 represents ineffectively confined region, dividing this volume by the total volume, one can get the approximate value of effectiveness ratio defined in Mander *et al.* (1988). According to the FE results of the current model, the calculated effectiveness ratios using the above mentioned method for three different pitches 13mm, 26mm and 39mm are 0.906, 0.846 and 0.761, while the corresponding effectiveness ratios calculated by Mander *et al*. (1988) method are 0.929, 0.849 and 0.772. The differences are 2.5%, 0.4% and 1.4%, respectively. This indicates that the FE model can closely predict the effectiveness ratio using the concept of arching action and effectively confined volume proposed by Mander *et al.* (1988).

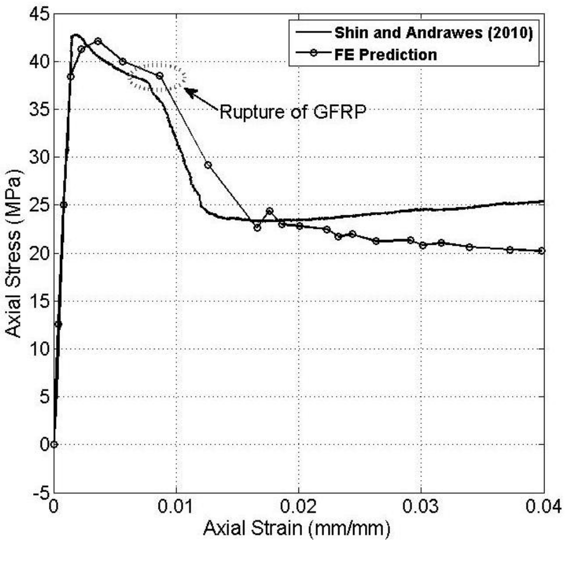

Figure 9. FE prediction of GFRP-SMA confined concrete compared with experimental result

4.2.2. GFRP-SMA hybrid confinement

Fig. 9 shows axial stress-strain curve of GFRP-SMA confined concrete test result compared with FE prediction. The proposed model can capture peak strength and closely predict the rupture of GFRP jacket. The peak stress from FE prediction is 42.1 MPa, while the experimental result is 42.8 MPa (1.6% difference). After GFRP ruptures, axial stress in experimental result drops abruptly and increases gradually afterward, while the FE result shows a slightly decreasing branch. However, the difference between the experimental and numerical results is deemed minor and the proposed model is found to be capable of closely predicting the behavior of GFRP-SMA confined concrete.

4.2.3. Comparison between SMA and GFRP-SMA confinements

Fig. 10 compares the average confining pressures across the height of concrete cylinder from SMA confined concrete model and that from GFRP-SMA confined concrete model. Step 0-1 is the initialization of active confining pressure and step 1-2 is compressive loading step. It shows average active confining pressure from SMA confinement is greater than that from GFRP-SMA confinement. This figure proves the reduced efficiency of SMA spirals when GFRP jacket is present between concrete and SMA spirals, which is consistent with the experimental results. During loading, passive confining pressure contributed from both GFRP jacket and SMA spirals makes average confining pressure in GFRP-SMA confinement greater than that in pure SMA confinement. After GFRP ruptures, average confining pressure reduces to a similar level as that of pure SMA confined concrete.

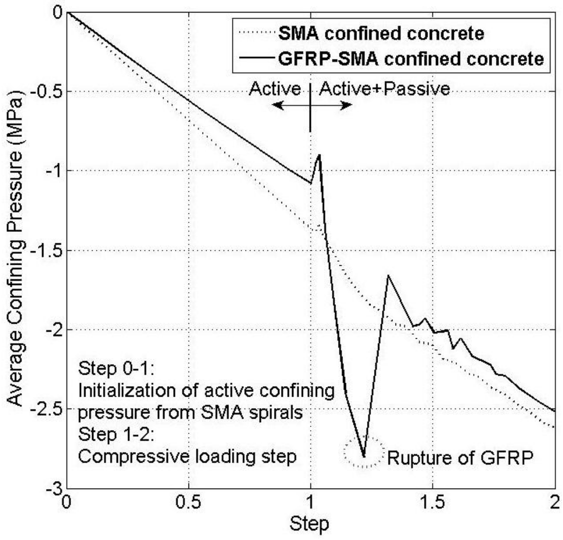

Figure 10. Comparison of average confining pressure from SMA confined concrete model and GFRP- SMA confined concrete model

5. CONCLUSIONS

This study focused on developing a finite element model within the framework of Concrete Damaged Plasticity Model in ABAQUS to predict the behavior of SMA confined concrete and GFRP-SMA confined concrete. The innovative feature of this model is that it is applicable to different kinds of confinement techniques, including SMA confinement and GFRP-SMA hybrid confinement. The yield criterion described in Lubliner *et al.* (1989) and modified in Lee and Fenves (1998) is used. A Drucker-Prager type potential flow is adopted. Sets of hardening/softening functions and dilation angle functions are calculated based on Mander *et al.* (1988) model. Different types of confinement exhibit different efficiency in improving the strength and ductility. Therefore, hardening/softening function and flow rule should not be only related to the lateral confining pressure, but also on the confinement technique used. In the hybrid case (GFRP-SMA), the presence of GFRP jacket between concrete and SMA spirals makes SMA spirals less efficient. An increased K_c factor is used to consider the effect of GFRP jacket before rupture. After rupture, SMA spirals contribute to concrete confinement directly and no modification of K_c factor is applied.

The proposed damaged plasticity model can closely predict the behavior of SMA confined concrete and GFRP-SMA hybrid confined concrete, including the peak strength, ascending/descending branch and the rupture of GFRP jacket. It shows that when active confinement is applied to the cylinder, core concrete is more confined than surface concrete and cover concrete starts to crack as axial loading becomes larger. In addition, the FE model is able to capture arching action and effectiveness ratio calculated using ineffectively confined volume as described by Mander *et al.* (1988). Furthermore, FE results show the average active confining pressure from GFRP-SMA confinement is greater than that from SMA confinement, resulting from the presence of GFRP jacket between concrete and SMA spiral, which reduces the efficiency of SMA spirals. FE model can also displays the contribution from both GFRP and SMA spirals on passive confining pressure in hybrid confinement, which exhibits greater average confining pressure than that from SMA confinement before GFRP ruptures and decreases to a similar level of average confining pressure as that from SMA confinement after GFRP ruptures. However, hardening/softening function and flow rule are both calculated based on actively confined concrete stress-strain curve developed based on high confining ratio (greater than 10%), while all the experiments done by Shin and Andrawes (2010) are in low confining ratio. Therefore, more experiments are needed to verify this modeling technique and a more generalized model can be developed based on more experimental results.

REFERENCES

ABAQUS. (2010). ABAQUS Analysis User's Manual, version 6.10.

Chun, S.S. and Park, H.C. (2002). Load carrying capacity and ductility of RC columns confined by carbon fiber reinforced polymers. *3rd Int. Conference on Composites in Infrastructure (CD-ROM).*

Jiang, T. and Teng, J.G. (2007). Analysis-oriented stress-strain models for FRP-confined concrete. *Eng. Struct.* **29:11**, 2968-2986.

Lee, J. and Fenves, G.L. (1998). Plastic-damage model for cyclic loading of concrete structures. *J. Eng. Mech.* **124:8**, 892-900.

Lubliner, J., Oliver, J., Oller, S., and Onate, E. (1989). A plastic-damage model for concrete. *Int. J. Solid Struct.* **25**, 299-329.

Mander, J. B., Priestley, M. J. N., and Park, R. (1988). Theoretical stress-strain model for confined concrete. *J. Struct. Eng.* **114:8**, 1804–1826.

Mirmiran, A. and Shahawy, M. (1996). A new concrete-filled hollow FRP composite column. *Composites, Part B.* **27:3-4**, 263-268.

Oh, B. (2002). A plasticity model for confined concrete under uniaxial loading. Ph.D. thesis. Lehigh University.

Richart, F. E., Brandtzaeg, A., and Brown, R. L. (1928). A study of the failure of concrete under combined compressive stresses. *Rep. No. 185*, Univ. of Illinois Engineering Station, Urbana, Ill.

Schickert, G. and Winkler. H. (1977). Results of test concerning to multiaxial compressive stresses. *Deutscher Ausschuss für* Stahlbeton. Heft 277, Berlin, Germany.

Shin, M. and Andrawes, B. (2010). Experimental Investigation of Actively Confined Concrete Using Shape Memory Alloys. *J. Eng. Struct.* **32:3**, 656-664.

Shin, M. and Andrawes, B. (2011). Seismic repair of RC bridge piers using shape memory alloys. *ASCE Conference.* **Vol 401:** 2056 -2065.

Teng, J.G., Huang, Y. L., Lam, L., and Ye, L.P. (2007). Theoretical model for fiber reinforced polymer-confined concrete. *J. of Compos. Constr.* **11:2**, 201-210.

William, K. J., and Warnke, E. P. (1975). Constitutive model for the triaxial behavior of concrete. *Proc. Int. Association for Bridge and Struct. Eng.***19**, 1-30.

Xiao, Y. and Wu, H. (2000). Compressive behavior of concrete confined by carbon fiber composite jackets. *J. Mater. Civ. Eng.***12:2**, 139-145.

Yu, T., Teng, J.G., Wong, Y.L., and Dong, S.L. (2010). Finite element modeling of confined concrete-I: Drucker-Prager type plasticity model. *Eng. Struct.* **32:3**, 665-679.

Yu, T., Teng, J.G., Wong, Y.L., and Dong, S.L. (2010). Finite element modeling of confined concrete-II: Plastic-damage model. *Eng. Struct.* **32:3**, 680-691.